

ORIGINAL ARTICLE



Metabolomic Study on the Treatment of Herpangina with Acupuncture Trial

Shi-qi Liu^{1,2+}, LiChen²⁺, Xiao-jun Gou^{1,2,*}, Jun-li Yao^{2*}

¹Central Laboratory, Baoshan District Hospital of Integrated Traditional Chinese and Western Medicine, Shanghai 201999, China

²Pediatric Department, Baoshan Hospital Affiliated to Shanghai University of Traditional Chinese Medicine, Shanghai 201999, China

*Corresponding Author: Xiao-jun Gou, Jun-li Yao

Abstract

Aim This study aims to elucidate the mechanisms of acupuncture treatment for herpangina using metabolomic methods.

Background The condition known as herpangina, which predominantly affects children, is an upper respiratory system infection mainly triggered by enteroviruses, including Coxsackievirus A and EV-A71. It is highly prevalent in children, especially during the spring and summer, with transmission occurring via either the fecal-oral pathway or the respiratory system. The incidence rate is high among children, particularly those with compromised immune systems. The main symptoms include high fever, sore throat, refusal to eat, and excessive salivation, which can lead to impaired cardiopulmonary function in severe cases. Current treatment is mainly symptomatic, lacking specific drugs, and commonly includes ribavirin and interferon-alpha spray, which may have serious adverse reactions.

Methods This study included 19 patients with herpangina and 23 healthy subjects. The treatment group received conventional Western medicine symptomatic treatment plus acupuncture therapy, once daily for 3 days. The control group adhered to their regular activities, receiving no treatment. Glucose level measurements were taken initially and again following 3 days. Serum and urine samples were gathered initially and post-3-day period for non-targeted metabolomic analysis to study the metabolic profile differences between patients with herpangina and healthy subjects, as well as the metabolic changes in patients before and after acupuncture therapy.

Results Compared with the control group, patients with herpangina exhibited metabolic disorders in purine, glyoxylate and dicarboxylic acids, and amino acids (arginine, histidine, and proline), including 19 differential metabolites in serum and 36 in urine. Pathway analysis indicated that histidine metabolism and the metabolism of arginine and proline are the main pathways through which acupuncture treats herpangina.

Conclusions Patients with herpangina exhibit significant disruptions in purine, glyoxylate, dicarboxylic acid, and amino acid metabolism. Acupuncture therapy significantly modulates the metabolic pathways within the patient's body, particularly impacting the metabolism of histidine, arginine, and proline, thereby playing a role in treating herpangina.

Keywords: Herpangina, Acupuncture Therapy, Metabolomic Analysis, Histidine metabolism, Arginine and proline metabolism, amino acid metabolism.

Introduction

Herpangina, a form of acute respiratory infection in pediatric patients, is predominantly induced by enteroviruses, notably Coxsackievirus A,

Enterovirus A71 (EV71), and Echovirus strains.[1-3]. Spring and summer are the high-incidence seasons for this disease, which is

contagious[4]. Children with compromised immune function are more susceptible to viral infections, hence they have a higher incidence rate. Herpangina primarily spreads through the fecal-oral route or respiratory transmission. The virus invades the respiratory and gastrointestinal mucosa through the nasopharynx and oral cavity, where it lingers and replicates in the mucosal epithelial cells as well as the lymphatic tissues of the pharynx or intestine, then is released into the bloodstream, causing a series of inflammatory responses in the corresponding tissues and organs[5]. The main clinical manifestations include sudden high fever with recurrent episodes, sore throat, refusal to eat, excessive salivation, headache, vomiting, etc., with congested and inflamed pharynx and grayish-white vesicles[6]. If timely and effective treatment is not provided, it may lead to impaired cardiopulmonary function, and even cause febrile convulsions and seizures, severely affecting the child's health. Management of herpangina primarily focuses on alleviating symptoms, as no potent antiviral medications targeting enteroviruses are currently available[7-8]. Ribavirin and interferon alpha spray are often used for treatment[9-10], but they have severe adverse reactions, so it is necessary to look for alternative treatment methods.

Herpangina in children, in terms of clinical manifestations, is categorized in Traditional Chinese Medicine (TCM) as "oral ulcers" and "wind-heat pharyngitis." In the Qing Dynasty, Zheng Meijian described in "Chonglou Yuyue": "By using acupuncture to dredge the meridians and collaterals, the qi and blood can flow smoothly... This is the secret of treating wind-heat in the throat, and its efficacy is beyond words"[11]. This provides theoretical and practical experience for the acupuncture treatment of herpangina in children. In China, acupuncture is widely used to treat upper respiratory tract infections[12]. As a mature and applicable traditional Chinese medical technique with no obvious adverse reactions[13], acupuncture has gradually become one of the emerging therapies for treating herpangina in children. Nevertheless, the current research into the specific mechanisms underlying acupuncture's effects is quite limited, and the experimental methods that have been employed are somewhat outdated, which in turn restricts further investigation into the use of acupuncture for the treatment of herpangina.

Therefore, this study proposes that acupuncture treatment has a significant impact on herpangina, which is beneficial for the recovery of patients' biochemical indicators.

In clinical research, the primary application of metabolomics is the identification of biomarkers associated with diseases. Metabolomics is categorized into non-targeted and targeted approaches, and it is a scientific discipline that investigates the types, quantities, patterns of variation, and interactions of small molecule metabolites (<1500 Da) within a biological system following stimulation or perturbation and explores their relationship with physiological and pathological changes[14-16]. The research process encompasses sample preparation, application of metabolomic techniques, data analysis, and identification of metabolites and metabolic pathway analysis. The main advantage of non-targeted metabolomics lies in its broad coverage of metabolites. Unlike targeted metabolomics, which requires the prior selection of specific metabolites or pathways for analysis, non-targeted metabolomics provides comprehensive metabolic information by simultaneously detecting and analyzing many metabolites within an organism. Therefore, in this study, UHPLC-HRMR/MS was utilized to detect serum and urinary metabolites. Pattern recognition methods were employed to identify characteristic metabolites in the serum and urine of children with herpangina. This approach is expected to offer insights for further exploration of the potential mechanisms of acupuncture in treating herpangina in children within prospective metabolomic studies.

2. Materials and Methods

2.1 Ethical approval and trial registration

The Ethics Committee at Baoshan Hospital, which is part of Shanghai University of Traditional Chinese Medicine, granted approval for this research (approval number 202204). Additionally, the research protocol was successfully registered on the China Clinical Trial Registry website, under the registration number ChiCTR2300077459. Compliance with the Declaration of Helsinki's ethical standards was maintained throughout the study's design and execution. Prior to their involvement, all subjects

provided their written consent after being fully informed.

2.2 Study Design

The study was executed in the form of a non-blinded, three-group, randomized clinical trial, taking place at the Baoshan District Hospital specializing in the integration of Traditional Chinese and Western medicine, located in Shanghai, China. A total of 20 patients with herpangina (with 1 case dropping out after treatment) and 23 healthy subjects were recruited to examine the changes in their serum and urinary metabolomic profiles. The mean age of the pre-treatment group was 4.75 ± 1.37 years, with a gender ratio of 12 males to 8 females. Post-treatment, the mean age was 4.32 ± 1.16 years, and the gender ratio was 12 males to 7 females. The control group had a mean age of 5.91 ± 1.20 years, with a gender ratio of 12 males to 11 females. There were no statistically significant differences in age and gender among the three groups.

2.3 Study Participants

Participants were recruited from October 2022 through August 2023. Patients with herpangina and healthy subjects who met all of the following criteria were included in the study.

Eligibility and Recruitment Criteria for Participants:

Patients with herpangina:

(1) Inclusion Criteria: ①Meet the diagnostic criteria for pediatric herpangina according to Western medicine; ②Ages between 1 to 7 years old; ③Duration of illness less than 3 days; ④Negative for antibodies in the novel coronavirus pneumonia nucleic acid test; ⑤The parents or legal representatives grant permission after being fully informed, ensuring the child's participation in the treatment process, and a document of consent is duly executed.

(2) Exclusion Criteria: ①Those with concurrent heart, liver, kidney dysfunction, coagulation mechanism disorders, or complications; ②Individuals allergic to Western medicines used in this study; ③Those who experience needle fainting; ④Individuals with skin inflammation or damage at the acupoint site; ⑤Pediatric patients presenting with vesicular eruptions on their palms

and soles, as well as those diagnosed with hand, foot, and mouth (HFMD) disease; ⑥Individuals with spontaneous bleeding or coagulation dysfunction.

Control Group Participants: Individuals who are in good health, matching the demographic characteristics of patients afflicted with herpangina in terms of age, gender, and ethnicity, and are free from any significant medical conditions, both structural and functional, were enlisted to form the control cohort.

2.4 Interventions

Treatment Group: The treatment regimen included conventional Western medical symptomatic treatment (antipyretic, anticonvulsant, and oral cefuroxime axetil suspension for anti-infection when needed) plus bloodletting therapy at specific acupoints (Si Feng, Shao Shang, and ear apex points), administered once daily for a continuous period of 3 days.

Healthy Control Group: No additional interventions were applied. Participants underwent routine examinations and information was collected promptly.

2.5.1 Sample Collection and Preparation

The acupuncture intervention group had samples collected at baseline and post-intervention, while the healthy control group had samples collected only at baseline. Approximately 20 mL of urine samples were collected in standard urine cups from patients before and after the bloodletting therapy, and approximately 5 mL of venous blood was also collected. For non-targeted metabolomic analysis, the urine and blood samples were allowed to stand for 1 hour at 4°C before being centrifuged at 3,000 rpm for 10 minutes. Subsequently, the supernatant samples were divided into portions and placed into 1.5 mL Eppendorf tubes, followed by preservation at a temperature of -80°C Celsius for subsequent applications.

2.5.2 Serum Sample Preparation

After thawing at 4°C, 100 μ L of serum was taken and placed into a 2 mL centrifuge tube, followed by the addition of 400 μ L of pre-chilled methanol (1:4, v:v), and vortexed for 60 seconds. After centrifugation at 4°C at 12,000 rpm for 10 minutes, the entire supernatant was transferred to a 2 mL centrifuge tube and vacuum concentrated

to dryness. The remaining solid was dissolved in 150 μL of an L-2-chlorophenylalanine solution prepared in 80% methanol, and the supernatant was filtered through a 0.22 μm pore size needle-type filter to obtain the serum sample ready for instrumental analysis.

2.5.3 Urine Sample Preparation

After thawing at 4°C, 200 μL of urine was taken and placed into a 5 mL centrifuge tube, followed by the addition of 1.7 mL of methanol and 60 μL of heptanoic acid (0.2 mg/mL) as an internal standard, and vortexed for 60 seconds. After centrifugation at 4°C for 10 minutes, 1.5 mL of the supernatant was transferred to a 2 mL centrifuge tube and vacuum concentrated to dryness. The residue was reconstituted in 60 μL of a 20 mg/mL solution of methoxy pyridine hydrochloride, vortexed for 30 seconds, and then reacted at 37°C for 2 hours. To the above solution, 60 μL of BSTFA reagent (containing 1% trimethylchlorosilane) was added, and the mixture was reacted at 37°C for 90 minutes. After centrifugation at 4°C at 12,000 rpm for 10 minutes, the supernatant was filtered through a 0.22 μm pore size needle-type filter. The filtrate was mixed with an equal volume of the internal standard to obtain the sample for detection.

2.6 Instrumental Analysis Conditions

2.6.1 UHPLC-HRMR/MS Conditions

2.6.1.1 Liquid Phase Conditions

The separation of the samples was achieved through the application of an ultra-high-performance liquid chromatography setup, the model Ultimate 3000 from Thermo Fisher Scientific, in conjunction with an ACQUITY UPLC BEH C18 column (2.1 mm \times 100 mm, 1.7 μm , Waters). The column temperature was maintained at 50°C with a flow rate of 0.35 mL/min for gradient elution. In positive ion mode, the injection volume for serum was 2 μL and for urine was 1 μL . The mobile phases consisted of 0.1% formic acid in water (Solvent A) and 0.1% formic acid in methanol (Solvent B). The gradient elution program was as follows: 0–2 min, 1% B; 11 min, 100% B; 13 min, 100% B; 13.2 min, 1% B; 15 min, 1% B. In negative ion mode, the injection volume for both serum and urine was 3 μL . The mobile phases consisted of water (Solvent A) and methanol (Solvent B), both containing 6.5 mM ammonium bicarbonate. The

gradient elution process was: 0 min, 1% B; 10 min, 100% B; 12 min, 100% B; 12.2 min, 1% B; 14 min, 1% B.

2.6.1.2 Mass Spectrometry Conditions

The mass spectrometry of metabolites was conducted using a Q Exactive Orbitrap mass spectrometer. For the ionization process, a heated electrospray ionization source (HESI) was applied to metabolites, operating in both the positive and negative ionization modes. The main parameters for the ion source were set as follows: the spray voltage was 3.8 kV for positive ions and 3.2 kV for negative ions, the capillary temperature was 320°C, and the auxiliary gas heater temperature was 350°C. The sheath gas flow rate was set at 40 (arbitrary units), and the auxiliary gas flow rate was set at 10 (arbitrary units). The S-Lens RF level was set at 50 (arbitrary units). The full-scan mass range for the first-level mass spectrometry was from m/z 70 to 1050, with a resolution of 35,000 at m/z 200, and an AGC target of 3×10^6 . Data-dependent acquisition (DDA) mode was used to collect the MS/MS fragment information of up to 6 parent ions per scan cycle. Higher-energy collisional dissociation (HCD) was employed for secondary fragmentation, with collision energies set at 15, 30, and 45 eV (NCE). The resolution for the second-level mass spectrometry was 17,500, and the AGC target was 1×10^5 .

2.7 Data Processing and Pattern Recognition Methods

The raw LC-MS data files obtained from both positive and negative ion modes were converted into NetCDF format using the Protowizard software (v3.0.8789). Subsequently, the R package XCMS (v3.3.2) was utilized for peak identification, peak filtering, and peak alignment. Ultimately, a data matrix containing information on mass errors, retention times, peak areas, and other details was generated. The acquired data were normalized and then imported into SIMCA software (V14.1) for multivariate statistical analysis. Principal component analysis (PCA) was employed to reveal the overall distribution of the metabolic profiles of samples across different groups. OPLS-DA modeling was used to generate S-plot diagrams and weight coefficients (VIP > 1). Metabolites were selected through univariate validation (T-TEST, $P < 0.05$), and the precise

metabolite information was further compared in the HMDB (Human Metabolome Database). The analysis of metabolic pathways was conducted employing the MetaboAnalyst 6.0.

2.8 Statistical Analysis

For clinical data, analysis was performed using the SPSS 21.0 statistical software. Quantitative data that conform to a normal distribution are expressed as the mean \pm standard deviation, and independent sample t-tests were used to analyze differences between groups. Categorical data are represented as frequencies (or rates), and chi-square (χ^2) tests were employed for group comparisons, with a P-value of less than 0.05 (two-tailed) considered to indicate statistically significant differences.

Metabolomic data were analyzed using univariate analysis with paired t-tests ($p < 0.05$) and multivariate analysis, including unsupervised

principal component analysis (PCA) and orthogonal partial least squares discriminant analysis (OPLS-DA). Variable importance in projection (VIP) values was used as an auxiliary screening criterion, with a VIP greater than 1 as the standard for selection.

3 Results

3.1 Demographic Information

Enrollment for this investigation included 20 patients diagnosed with herpangina, with the exception of one who withdrew following acupuncture intervention, and 23 healthy volunteers. Comparative evaluation of various parameters did not yield any marked disparities between the herpangina-afflicted group and the healthy control cohort. A comprehensive overview of the demographic profiles of these participants can be found in Table 1.

Tab.1 Demographic information ($\bar{x} \pm s$)

Characteristics		pre-treatment group (n=20)	post-treatment group (n=19)	Control group (n=23)	
Age (years)		4.75 \pm 1.37	4.32 \pm 1.16	5.91 \pm 1.20	
Sex	male, n (%)	12 (60%)	12 (63%)	12 (52%)	
	female, n (%)	8 (40%)	7 (37%)	11 (48%)	
Serological immunity (g/L)	IgA	1.09 \pm 0.48	1.20 \pm 0.44	1.27 \pm 0.84	
	IgM	1.18 \pm 0.35	1.09 \pm 0.42	0.99 \pm 0.37	
	IgG	8.62 \pm 1.47	9.19 \pm 2.01	9.14 \pm 2.01	
	IgE	180.22 \pm 282.10	149.63 \pm 280.65	345.77 \pm 877.14	
Enteroviruses	Coxsackievirus A16 IgM Antibody	Negative, n (%)	18 (90%)	18 (95%)	23 (100%)
		Positive, n (%)	2 (20%)	1 (5%)	0 (0%)
	Enterovirus 71 IgM Antibody	Negative, n (%)	20 (100%)	19 (100%)	23 (100%)
		Positive, n (%)	0 (0%)	0 (0%)	0 (0%)

3.2 Metabolomics Studies

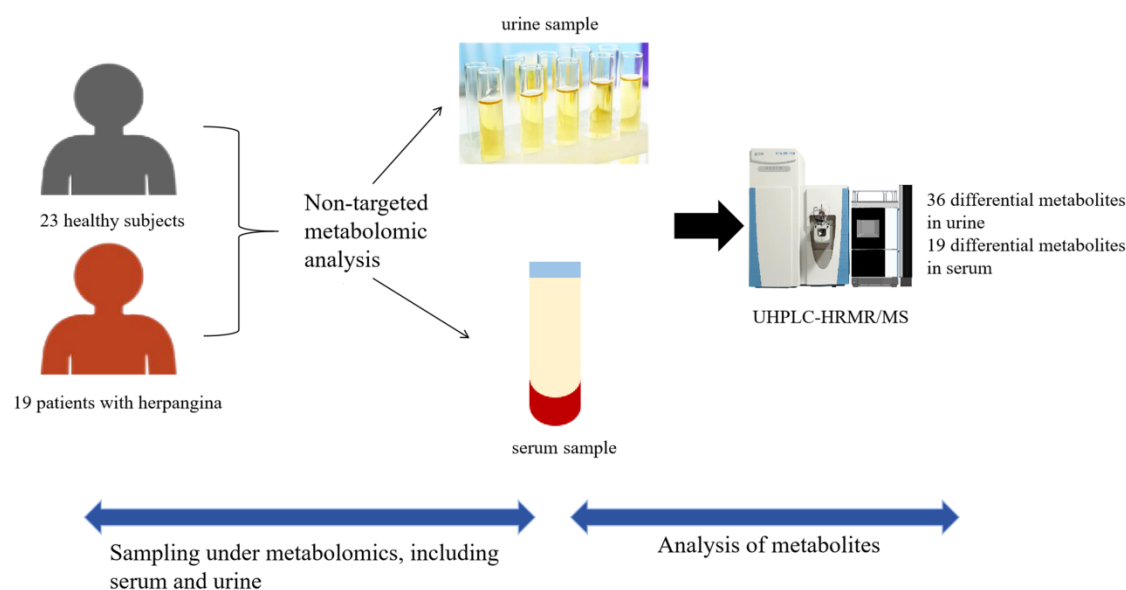
3.2.1 Metabolic Profile Analysis

Unsupervised PCA was employed to assess the overall distribution of the metabolomic profiles, with the aim of identifying any outliers. Figures (1A, C, E, and G) demonstrate that the metabolic profiles of the control group and the pre-treatment group cluster closely together, indicating insufficient separation. To further examine the metabolic disruptions in patients with herpangina, a more detailed analysis using OPLS-DA modeling is warranted.

The results from both serum and urine samples reveal a clear separation between the groups, with high values for both the goodness of fit (R^2) and the predictability (Q^2) prior to treatment. These findings are illustrated in Figures (1B, D, F, and H) and detailed in Table 2. The effective separation observed in the metabolic profiles post-treatment suggests that the therapeutic intervention had a significant impact on the metabolomic landscape of the patients with herpangina.

Tab. 2 Model Parameters

Model type	R2X	R2	R2Y	Q2
Serum-anion	0.667	0.923	1	0.51
Serum-cation	0.901	0.833	1	0.754
Urine-anion	0.895	0.974	1	0.435
Urine-cation	0.643	0.633	1	0.349



Metabolomic analysis of serum and urine samples from patients with herpes pharyngitis

Graphical Abstract

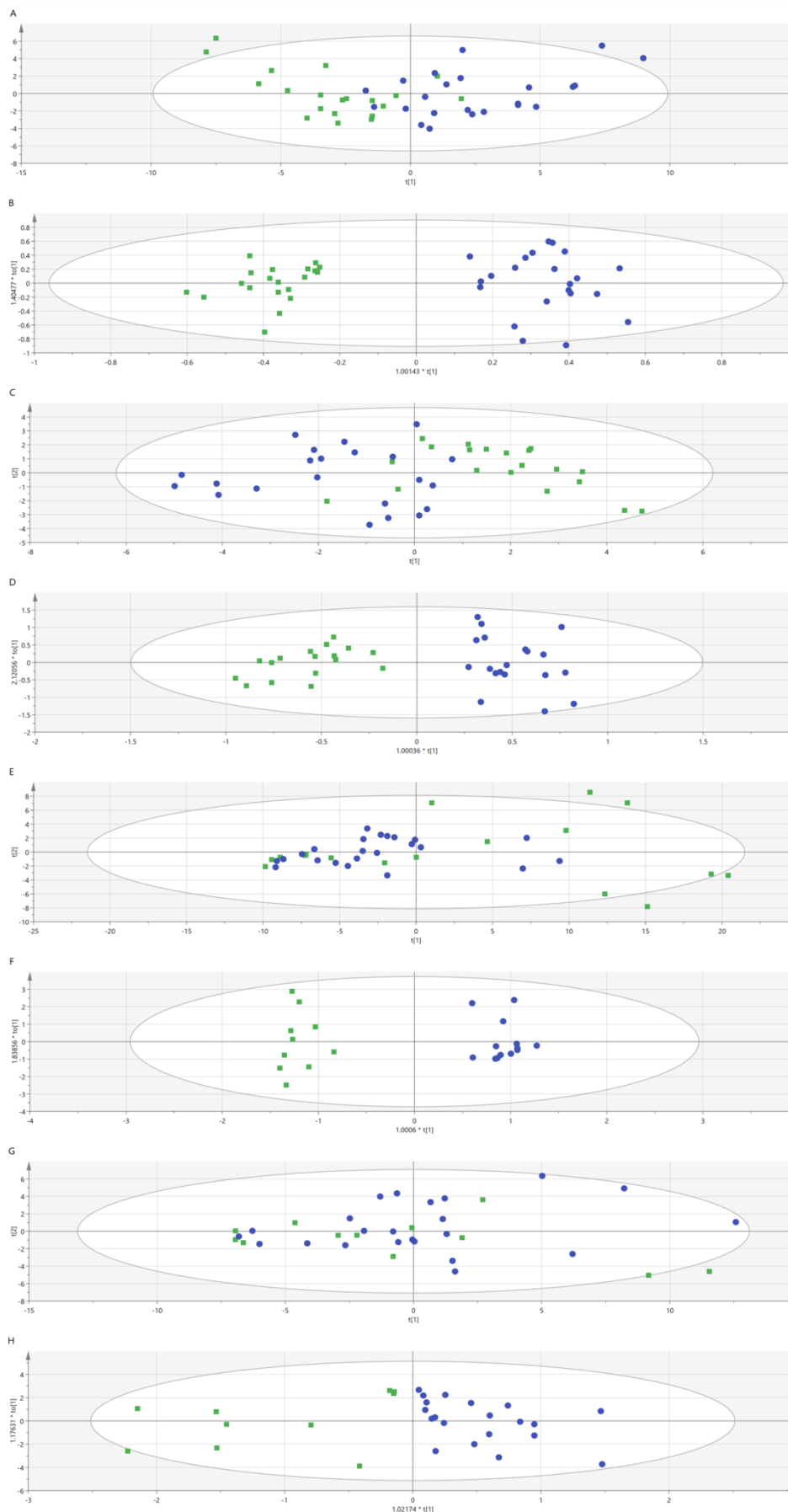


Fig. 1 Metabolic scores of the control and pre-treatment groups are plotted. Serum: (A)PCA for anions, (B)OPLS-DA for anions, (C)PCA for cations, (D)OPLS-DA for cations; Urine: (E)PCA for anions, (F)OPLS-DA for anions, (G)PCA for cations, (H)OPLS-DA for cations. ■ pre-treatment group, ● control group

3.2.2 Differential Metabolite Screening

In the OPLS-DA pattern recognition, differential metabolites were screened using the criteria of $VIP > 1$ and $P < 0.05$. The Splot diagram indicates

that points farther from the center are more likely to be differential metabolites (Figure 2).



Fig. 2 Splot plots of control and pre-treatment groups. A: serum-anion, B: serum-cation, C: urine-anion, D: urine-cation

Ultimately, 19 differential metabolites were identified in serum and 36 differential metabolites in urine. These differential metabolites are

associated with herpangina, and the results are presented in Tables 3-4.

Table 3 Metabolites in serum samples from control and pre-treatment groups

Metabolite	mz	Rt(min)	VIP value	Comparison between pre-treatment group and control group		Comparison between Post-treatment group and pre-treatment group	
				p value	Change trend (pre-treatment group/control group)	p value	Change trend (Post-treatment group/pre-treatment group)
Inosine	267.07	2.24	3.08	0.0077	0.39↓	0.7823	0.90↓
L-Arginine	173.10	0.80	2.73	0.0002	0.69↓	0.9732	1.00↑
L-Lysine	145.10	0.80	1.83	0.0012	0.76↓	0.0513	1.28↑
4-	199.01	5.86	1.67	0.0054	0.49↓	0.2156	1.41↑

vinylphenol sulfate							
octadecadienoic acids	671.47	13.64	1.67	0.0469	0.60↓	0.2305	1.40↑
L-Histidine	154.06	0.78	1.64	0.0181	0.83↓	0.0615	1.21↑
Erucic acid	337.31	12.26	1.58	0.0218	3.03↑	0.7032	0.84
Glutamine	145.06	0.73	1.53	0.0075	0.72↓	0.9985	1.00↑
24S-hydroxycholesterol 3-sulfate, 24-D-glucuronide	328.16	9.57	1.52	0.0188	1.93↑	0.0906	0.62↓
Glycolithocholic acid 3-sulfate	255.63	9.12	1.50	0.0388	2.57↑	0.9116	1.05↑
2,6-Dihydroxybenzoic acid	153.02	4.34	1.49	0.0435	0.59↓	0.3505	1.29↑
Taurolithocholic acid 3-sulfate	280.62	9.11	1.47	0.0173	4.35↑	0.3523	0.65↓
Ornithine	131.08	0.79	1.43	0.0103	0.78↓	0.0777	1.20↑
Merochlorin C	246.07	6.51	1.36	0.0322	2.27↑	0.4164	0.75↓
Chenodeoxycholic acid	391.29	9.28	1.25	0.0168	0.45↓	0.4285	1.36↑
Gibberellin A12	331.19	8.47	1.05	0.0010	2.28↑	0.1993	0.75↓
Hypoxanthine	137.05	1.80	3.88	0.0255	0.50↓	0.6480	0.64↓
Acetyl-L-carnitine	204.12	0.94	2.12	0.0390	1.36↑	0.4200	1.13↑
Methionine	150.06	1.07	3.56	0.0183	0.81↓	0.0168	0.44↓

Table 4 Metabolites in urine samples from control and pre-treatment groups

Metabolite	mz	Rt(min)	VIP value	Comparison between pre-treatment group and control group		Comparison between Post-treatment group and pre-treatment group	
				p value	Change trend (pre-treatment group/control group)	p value	Change trend (Post-treatment group/pre-treatment group)
Pseudouridine	243.06	1.03	3.98	0.0084	3.49↑	0.1178	0.58↓
Actinozine A	241.12	4.60	3.47	0.0446	2.58↑	0.2291	0.61↓
leucyl-4-hydroxyproline	243.13	5.08	3.11	0.0131	4.25↑	0.1017	0.48↓
4-Oxoproline	128.04	0.77	3.08	0.0302	3.84↑	0.0553	0.61↓
2-Hydroxyethanesulfonate	124.99	0.73	2.36	0.0174	3.54↑	0.0954	0.64↓

Urocanic acid	137.04	2.98	2.12	0.0242	3.52↑	0.0464	0.66↓
Hypoxanthine	135.03	1.16	2.01	0.0496	2.78↑	0.0903	0.62↓
cis-Aconitic acid	173.01	0.63	1.84	0.0242	4.70↑	0.0708	0.63↓
3-Furoic acid	129.02	0.63	1.84	0.0339	4.53↑	0.0727	0.63↓
Alanopine	160.06	0.84	1.76	0.0265	3.86↑	0.0704	0.56↓
Dihydrouridine	245.08	1.09	1.72	0.0239	3.22↑	0.1620	0.63↓
Cladosin L	269.15	6.80	1.70	0.0200	4.14↑	0.1082	0.43↓
DL-Arabinose	149.05	0.76	1.68	0.0497	3.97↑	0.9441	1.03↑
3-(1H-imidazol-5-yl)-2-oxopropionic acid	153.03	1.03	1.66	0.0123	3.45↑	0.1340	0.60↓
N-[(3s)-2-Oxotetrahydrofuran-3-yl]butanamide	170.08	4.79	1.57	0.0300	2.35↑	0.1173	0.59↓
Penicilpyranone	199.10	1.54	1.45	0.0466	4.20↑	0.1181	0.47↓
N ² ,N ² -Dimethylguanosine (incorrect stereochemistry)	310.12	4.35	1.39	0.0265	3.32↑	0.1170	0.67↓
Lorbamate	257.15	6.00	1.33	0.0376	2.85↑	0.0490	0.37↓
(3R,5R)-3,5-dihydroxydecanoic acid	203.13	5.92	1.26	0.0351	3.76↑	0.0791	0.49↓
Pestalachloride C	421.06	7.30	1.23	0.0392	10.96↑	0.0776	0.12↓
Hexanoylglycine	172.10	5.14	1.22	0.0244	2.93↑	0.0773	0.54↓
Ecgonine methyl ester	198.11	7.21	1.08	0.0068	3.54↑	0.0494	0.47↓
Glutamine	145.06	4.60	1.06	0.0438	2.61↑	0.1966	0.60↓
(Z)-3-hydroxydodec-5-enoic acid	213.15	9.11	1.06	0.0260	3.24↑	0.0906	0.52↓
5-Hydroxytryptophan	219.08	1.61	1.03	0.0428	3.17↑	0.2588	0.76↓
Ascorbic acid	193.04	0.70	1.02	0.0213	2.95↑	0.0210	0.50↓
3-[(2,6-Dimethylheptanoyl)oxy]-4-(trimethylammonio)butanoate	302.23	8.06	5.04	0.0469	0.59↑	0.8131	1.05↑
Cytosine	112.05	1.47	2.39	0.0184	3.25↑	0.6983	0.85↓
5-(2-Methylpropyl)-3,6-dioxo-2-piperazinepropanoic acid	243.13	6.37	1.87	0.0195	2.43↑	0.2929	0.69↓
10-Nitrooleic acid	328.25	8.58	1.62	0.0435	2.80↑	0.0470	0.34↓
Metipranolol	310.20	7.68	1.59	0.0311	1.81↑	0.1876	0.67↓
pentahomomethionine	220.14	7.30	1.55	0.0452	2.10↑	0.0625	0.47↓
4,4'-Thiobis-2-butanone	175.08	5.60	1.53	0.0440	2.33↑	0.2349	0.62↓
trihomomethionine	192.10	5.61	1.25	0.0351	2.32↑	0.2263	0.64↓

2-Amino-2-(2-methylenecyclopropyl)acetic acid	128.07	1.87	1.22	0.0498	2.16↑	0.4639	0.75↓
9-Decenoylcarnitine	314.23	8.25	1.02	0.0474	1.73↑	0.0505	0.54↓

3.2.3 Effects of acupuncture treatment on metabolic profiles and differential metabolites

3.2.3.1 Effects on metabolic profiles and differential metabolites in serum

Supervised OPLS-DA was utilized to profile the serum metabolomics across three distinct groups: the control, the pre-treatment, and the post-treatment. The results indicated that the metabolic profiles of the acupuncture group before treatment

were markedly different from those of the control group, and the profiles after treatment deviated from those of the acupuncture group before treatment. Furthermore, as shown in Table 5, the relative concentration trends of some metabolites changed, with 5 metabolites returning to normal levels after treatment. These findings are illustrated in Figures 1(B and D) and Figures 3(A and B).

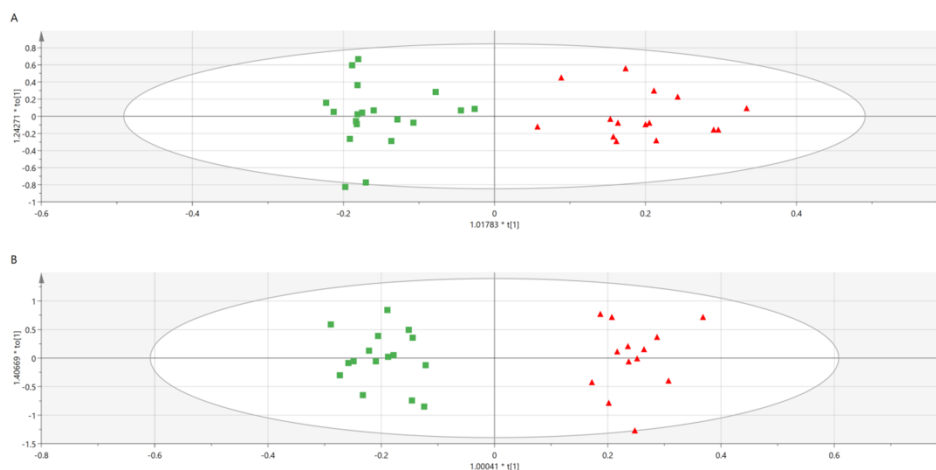


Fig. 3 Serum metabolic OPLS-DA scores in the pre-treatment and post-treatment groups

A: serum-anion, B: serum-cation. ■ pre-treatment group, ▲ Post-treatment group.

Table 5 Metabolites in serum samples from the pre-treatment and post-treatment groups

Metabolite	mz	Rt(m in)	VIP value	Comparison between pre-treatment group and control group		Comparison between Post-treatment group and pre-treatment group	
				p value	Change trend (pre-treatment group/control group)	p value	Change trend (Post-treatment group/pre-treatment group)
Methionine	150.06	1.07	3.56	0.0183	0.81↓	0.0168	0.44↓
DL-Lysine	147.11	0.63	1.85	0.0224	0.84↓	0.0335	0.17↓
(10E,12E)-9-oxooctadeca-10,12-dienoic acid	295.23	11.14	1.69	0.7533	0.95↓	0.0482	0.07↓

2-Methyl-4-propyl-1,3-oxathiane	159.08	8.38	1.41	0.0015	0.80↓	0.0086	1.19↑
15(S)-HPETE	339.25	9.35	1.27	0.0044	0.67↓	0.0162	1.34↑

3.2.3.2 Effects on Metabolic Profiles and Differential Metabolites in Urine

The application of supervised OPLS-DA metabolomics was employed for the examination of urine samples across three distinct groups. The results revealed that the metabolic profiles of the control group were markedly distinct from those

of the pre-treatment group, and the outcomes of the post-treatment group differed from those of the pre-treatment group. Additionally, as indicated in Table 6, the relative concentration trends of certain metabolites underwent changes, with 14 metabolites returning to normal levels after the intervention. These findings are depicted in Figures 1(F and H) and Figures 4(A and B).

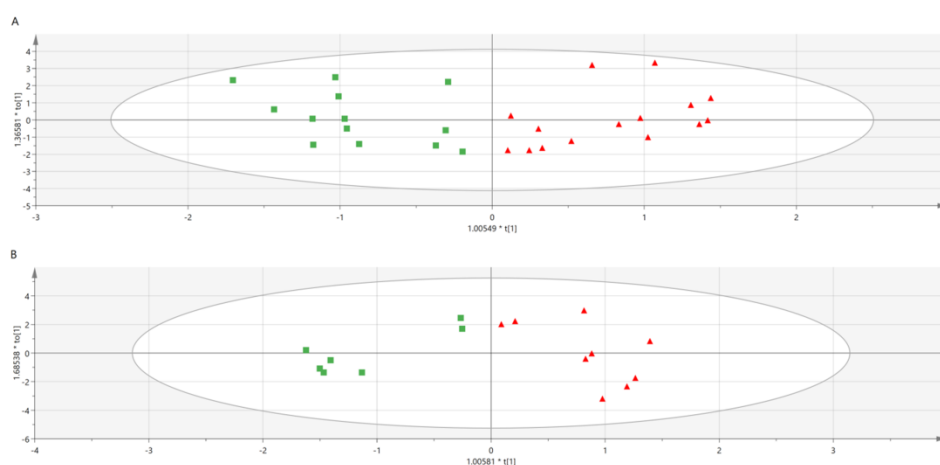


Fig. 4 Urinary metabolism OPLS-DA scores in the pre-treatment and post-treatment groups: A: urine-anion, B: urine-cation; ■ pre-treatment group; ▲ pre-treatment group,

Table 6 Metabolites in urine samples from the pre-treatment and post-treatment groups

Metabolite	mz	Rt(mi n)	VIP value	Comparison between pre-treatment group and control group		Comparison between Post-treatment group and pre-treatment group	
				p value	Change trend (pre-treatment group/ control group)	p value	Change trend (Post-treatment group/pre-treatment group)
Mannostatin A	178.05	4.34	4.54	0.0158	0.11↓	0.0329	9.47↑
4-Oxo-L-proline	146.05	0.77	3.19	0.1001	2.97↑	0.0180	0.43↓
Urocanic acid	137.04	2.98	2.23	0.0242	3.52↑	0.0464	0.66↓
N-[(3s)-2-Oxo-tetrahydrofuran-3-Yl] butanamide	170.08	4.09	1.94	0.0512	3.07↑	0.0024	0.51↓
Lorbamate	257.15	6.00	1.66	0.0376	2.85↑	0.0490	0.37↓
Hexanoylglycine	172.098	5.135	1.59	0.0969	2.66↑	0.0310	0.57↓

(3R,5R)-3,5-dihydroxydecanoic acid	203.13	7.10	1.49	0.7171	1.53↑	0.0441	0.50↓
Penicipyranone	199.10	1.28	1.46	0.0337	3.39↑	0.0362	0.56↓
Ecgonine methyl ester	198.11	7.21	1.21	0.0068	3.54↑	0.0494	0.47↓
Propionylcarnitine	216.12	6.12	1.19	0.0038	3.54↑	0.0273	0.44↓
Primarolide B	442.17	4.33	1.19	0.0205	0.17	0.0354	6.29↑
L-Proline	114.06	0.83	1.10	0.0137	3.56↑	0.0064	0.40↓
Imidazoleacetic acid	125.04	3.63	1.06	0.0300	3.01↑	0.0307	0.58↓
10-Nitrooleic acid	328.25	8.58	1.46	0.0435	2.80↑	0.0470	0.34↓

Note: ↑: indicates that the metabolite content of the group is higher than that of the control group, ↓: indicates that the metabolite content of the group is lower than that of the control group.

3.2.4 Implications for Metabolic Pathway Analysis

To further elucidate the metabolic distribution and therapeutic targets of acupuncture treatment for pediatric herpangina, we introduced the 19 potential biomarkers from serum and 36 potential biomarkers from urine into the online system

MetaboAnalyst 6.0 for metabolic pathway analysis. The top 6 metabolic pathways with $P < 0.05$ before and after treatment in the acupuncture group were identified as follows: (a) Arginine biosynthesis; (b) Histidine metabolism; (c) Purine metabolism; (d) Glyoxylate and dicarboxylate metabolism; (e) Arginine and proline metabolism; (f) Nitrogen metabolism, as shown in Figure 5.

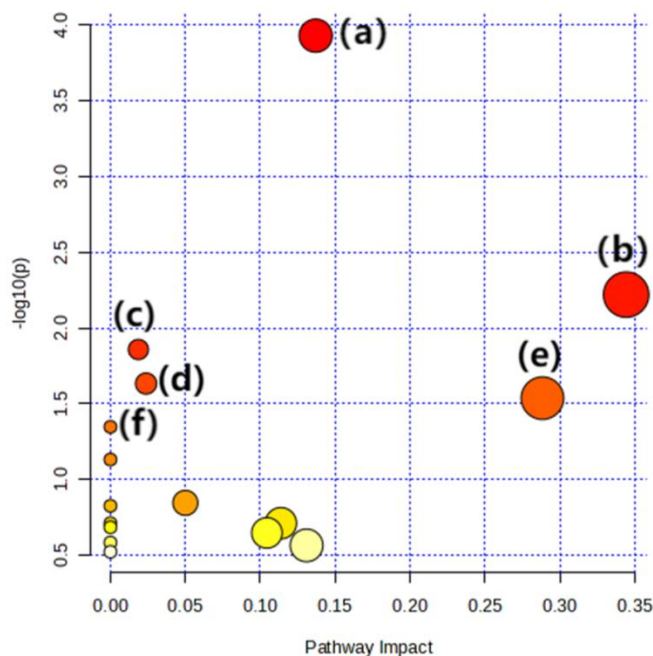


Fig. 5 Metabolic pathways associated with herpangina

(a)Arginine biosynthesis, (b)Histidine metabolism, (c)Purine metabolism, (d)Glyoxylate and dicarboxylate metabolism, (e)Arginine and proline metabolism, (f)Nitrogen metabolism

As indicated in Tables 5 and 6, metabolites in the treatment group that returned to normal levels with a change fold greater than 1.5 or less than 0.67 were subjected to metabolic pathway analysis using the online system MetaboAnalyst

6.0. In the treatment group, the metabolic pathways of (b) Histidine metabolism and (e) Arginine and proline metabolism were found to have normalized, as depicted in Figure 6.

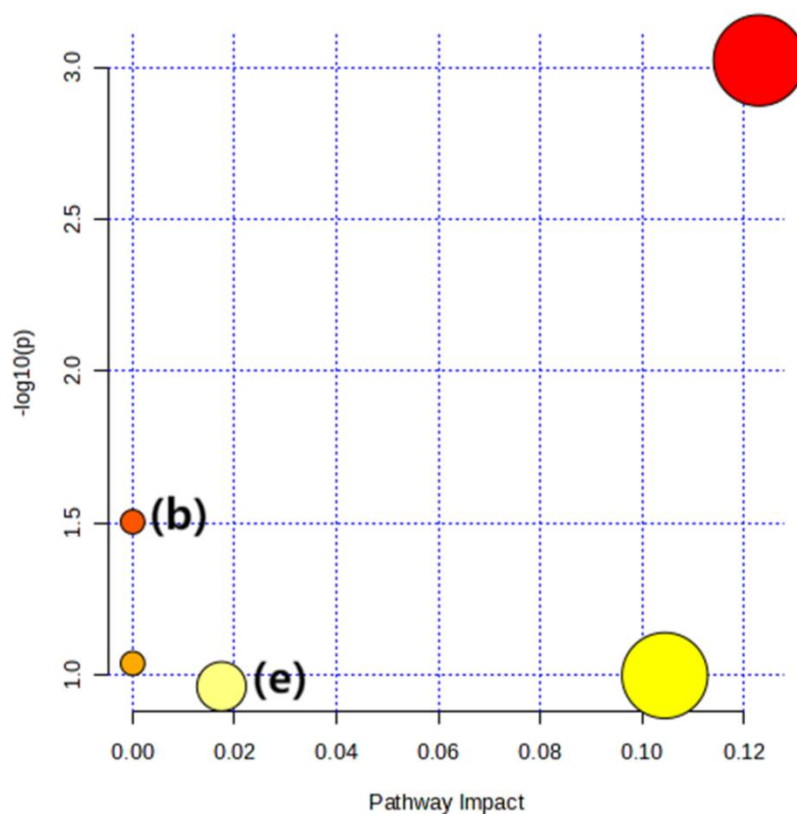


Fig. 6 Metabolic pathways associated with post-treatment groups
(b)Histidine metabolism, (e)Arginine and proline metabolism

4 Discussion

This study employs metabolomics to explore the impact of acupuncture on pediatric herpangina, representing a certain degree of innovation in this field. Utilizing non-targeted metabolomic analysis, this research examines the metabolic profiles of serum and urine samples from patients with herpangina, identifies differential metabolites and associated metabolic pathways, and investigates the effects of a 3-day acupuncture treatment on their metabolic health.

The results of the study indicate that there are significant differences in the metabolic profiles of serum and urine samples between patients with herpangina and healthy individuals. Following acupuncture intervention, the metabolic profiles of the post-treatment became similar to those of the control group, showing a trend toward

normalization. Furthermore, 19 and 36 biomarkers associated with herpangina were identified in serum and urine, respectively, with 19 of these metabolites returning to normal levels after treatment. These primarily involve metabolic pathways such as Histidine metabolism and Arginine and proline metabolism. This information enhances our comprehension of the etiology of herpangina as well as the processes that account for the beneficial outcomes of acupuncture treatment.

Metabolomic analysis revealed that compared to healthy individuals, patients with herpangina exhibit disruptions in purine metabolism and glyoxylate and dicarboxylate metabolism. Purines are among the most prevalent small molecule metabolites within cells and play a crucial role in neural regulation and transmission, cell

proliferation and differentiation, as well as energy metabolism[17]. Due to the involvement of purine nucleotides in a variety of cellular processes, even partial blockade of purine metabolism can lead to severe pathological and physiological consequences. The purine metabolic pathway involves the conversion of hypoxanthine to xanthine by xanthine oxidase, which is then further converted to uric acid[18]. Reactive oxygen species (ROS) induced by EV71 are essential for the replication of the virus within the host cells[19-20]. When the production of ROS exceeds the cell's antioxidant defense capabilities, oxidative stress (OS) ensues. Uric acid can act as a potent antioxidant, primarily maintaining the activity of peroxidases, preventing the excessive formation of superoxide compounds and peroxynitrites, and preserving cellular structure and function. Additionally, uric acid can chelate with iron ions to form complexes, thereby scavenging iron ions and reducing lipid peroxidation to alleviate oxidative load[21-22]. The results showed that children with herpangina had an increasing trend of hypoxanthine in their bodies, indicating a disruption in purine metabolism, affecting the production of uric acid, exacerbating oxidative stress, and consequently leading to inflammation and tissue damage.

The tricarboxylic acid (TCA) cycle, alternatively referred to as the citric acid cycle, functions as the ultimate metabolic route for the breakdown of carbohydrates, lipids, and amino acids, acting as a central node in their metabolic interconversion.[23]. Viruses necessitate the biosynthesis of lipids, proteins, and nucleic acids by their host cells to guarantee the formation of new viral offspring. Additionally, the host cells must generate energy to facilitate the assembly and dissemination of the virus. So it is essential for cellular energy acquisition and the viral replication cycle[24]. Macrophage metabolism produces numerous metabolic intermediates that play a crucial regulatory role in tissue repair and regeneration processes. Research has confirmed that the alteration of the TCA cycle is a pivotal aspect of metabolic reconfiguration associated with the polarization of macrophages.[25-26]. Pro-inflammatory macrophages (M1) rely primarily on glycolysis and the TCA cycle for their metabolic activities, while anti-inflammatory macrophages (M2) have an intact TCA cycle, enhance fatty acid oxidation, and depend on

oxidative phosphorylation[27-30]. Additionally, in energy metabolism, we observed disruptions in the metabolism of glyoxylate and dicarboxylic acids in patients with herpangina. This pathway is a shunt of the TCA cycle, capable of supplementing the insufficiency of certain intermediate metabolic products, and plays a major role in the metabolism of gut microbiota[31]. So The disruption in the glyoxylate and dicarboxylate metabolism observed in herpangina patients could indicate an impairment in the supplementary pathway of the TCA cycle, which may affect the energy production and the overall metabolic balance within the cells and potentially influence the host's immune response and cellular repair mechanisms.

Compared to healthy individuals, patients with herpangina exhibit significantly reduced levels of arginine, histidine, and lysine in serum, while proline levels are markedly increased in urine. Earlier investigations have shown that the metabolism of amino acids is capable of modulating the release of pro-inflammatory cytokines within macrophages.[32]. Essential to human nutrition, amino acids are vital for preserving the equilibrium of the immune system. A wealth of studies has demonstrated that a range of amino acids along with their byproducts, including histidine, arginine, and proline, have a significant impact on both the stimulation of immune cell activity and the release of inflammatory mediators.[33-35]. Enteroviruses, one of the significant causes of herpangina, can replicate in leukocytes, endothelial cells, and dendritic cells, leading to an over-release of inflammatory cytokines and chemokines that trigger a cytokine storm, forming severe disease complications that threaten life[36]. The interplay between the gut tissue and the microbial community, potentially outnumbering our own cells, is pivotal for digesting and metabolizing consumed food, regulating intestinal blood flow and vascular permeability, as well as managing inflammation[37-38]. Arginine, as a substrate for both intestinal and microbial cells[39], when affected by the virus, disrupts the symbiotic interaction between the gut tissue and the microbiota, altering the host's immune response and the composition of the gut microbiota. These changes can lead to metabolic disorders in the gut and increased intestinal permeability, thereby triggering inflammatory or infectious

diseases[40]. Histamine—a reactive molecule and an agent in inflammation—is produced from L-histidine through the catalytic activity of histidine decarboxylase (HDC), and it is sequestered within the granules of intracellular storage in both basophils and mast cells[41]. Upon the binding of antigen-IgE complexes to the FcεRI, which is the high-affinity IgE receptor present on basophil and mast cell surfaces, the sequestered histamine is swiftly discharged, leading to elevated local concentrations. The H4R, also known as the histamine H4 receptor, is predominantly found on immune-responsive cells such as mast cells, eosinophils, monocytes, dendritic cells, and T lymphocytes. The H4R facilitates the directional movement of immune cells, as well as triggering allergic and inflammatory responses; therefore, alleviating histidine metabolism disorders may help reduce the expression of H4R and mitigate inflammatory responses[42]. EV71, a prevalent pathogen responsible for herpangina, interacts with the scavenger receptor B2 (SCARB2), which serves as a principal receptor not only for EV71 but also for various other enteroviruses implicated in herpangina, and is vital in facilitating viral entry into cells.[43]. The 152-163 and 183-193 helices of SCARB2 dominate the interaction with the residues of the two major envelope proteins of EV71, VP1 GH, and VP2 EF loops. Nevertheless, it should be highlighted that numerous residues in the binding site are variable across enteroviruses reliant on SCARB2, whereas the conserved proline seems to play an essential role as a critical residue.[44-45]. Therefore, improving proline metabolism may aid in the treatment of herpangina. After acupuncture treatment intervention, the levels of arginine and histidine in serum returned to normal, and the levels of proline in urine were also corrected, thus promoting the normal metabolism of amino acids. The results indicate that after acupuncture intervention, the metabolism of histidine, arginine, and proline in patients with herpangina returned to normal, suggesting that the therapeutic mechanism of acupuncture may be related to the amino acid metabolism in patients with herpangina.

5. Conclusion

A UHPLC-HRMR/MS-based metabolomic approach was established to investigate the pathogenesis of herpangina and the therapeutic

effects of acupuncture. The results revealed that patients with herpangina exhibit impaired energy, fatty acid, and amino acid metabolisms. Acupuncture treatment was found to ameliorate the disrupted amino acid metabolism, suggesting its potential in regulating the metabolic disturbances associated with the disease. This method provides a valuable tool for understanding the metabolic perturbations in herpangina and the mechanisms underlying the therapeutic impact of acupuncture.

While this study integrates serum and urine metabolomics, which complement each other and lay the necessary foundation for further research on the application of acupuncture in treating herpangina, the results should be considered in light of the following limitations: a short treatment duration, a small sample size, uneven adaptability, and the absence of correlation analysis between metabolomics and clinical outcomes. Therefore, future studies will expand the sample size and further validate the research findings in both clinical and experimental settings. Despite these constraints, this study serves as a valuable reference for employing metabolomics to explore the mechanisms underlying the onset of herpangina. Additionally, the metabolic profiling of individual patients may inform the development of personalized treatment strategies for herpangina in the future.

Ethics Approval and Consent to Participate

This research protocol has been approved by the Ethics Committee of Baoshan Hospital Affiliated to Shanghai University of Traditional Chinese Medicine (Approval Number: 202204). The research protocol has been registered on the Chinese Clinical Trial Registry Platform (<http://www.chictr.org.cn/index.aspx>) with the registration number: ChiCTR2300077459.

Human and Animal Rights

This study is conducted strictly in accordance with the requirements of ethical approval, adhering to the ethical guidelines outlined in the "Regulations for Clinical Trials of Medical Devices," the "Declaration of Helsinki," and the "International Ethical Guidelines for Biomedical Research Involving Human Subjects."

Consent for Publication

Not applicable.

Funding

This study was financially supported by Project of Shanghai Municipal Science and Technology Commission (Project No.: 22Y11923300); Chen Li's Inheritance Studio of Famous Traditional Chinese Medicine Doctors in Baoshan District (Project No.: BSMZYGZS-2024-10).

Availability of Data and Materials

Not applicable.

Conflict of Interest

The authors declare that they have no conflicts of interest.

Acknowledgements

None declared.

Author Contributions

Shi-qi Liu and LiChen participated in the study design. Shi-qi Liu and LiChen analyzed the data and wrote the article. Jun-li Yao and Xiao-jun Gou reviewed the manuscript. All authors read and approved the final manuscript. Shi-qi Liu and LiChen contributed equally to this work and should be considered co-first authors. Jun-li Yao and Xiao-jun Gou contributed equally to this work and should be considered co-corresponding authors.

References

- Liang Z, Lin C, Huo D, et al. "First detection of multiple cases related to CV-A16 strain of B1c clade in Beijing in 2022," *Journal Of Medical Virology*, vol. 96, no. 7, pp. e29796, 2024.
- Wang Y, Gao F, Liang Z, Sun H, Wang J, Mao Q. "Establishment of the 1st Chinese national standard for CA6 neutralizing antibody," *Human Vaccines & Immunotherapeutics*, vol. 19, no. 1, pp. 2164140, 2023.
- Kang HJ, Yoon Y, Lee YP, et al. "A Different Epidemiology of Enterovirus A and Enterovirus B Co-circulating in Korea, 2012-2019," *Journal of the Pediatric Infectious Diseases Society*, vol. 10, no. 4, pp. 398-407, 2021.
- Yu H, Li XW, Liu QB, et al. "Diagnosis and treatment of herpangina: Chinese expert consensus," *World Journal of Pediatrics*, vol. 16, no. 2, pp. 129-134, 2020.
- Ye YZ, Dou YL, Hao JH, et al. "Efficacy and safety of interferon α -2b spray for herpangina in children: A randomized, controlled trial," *International Society for Infectious Diseases*, vol. 107, pp. 62-68, 2021.
- Corsino CB, Ali R, Linklater DR. "Herpangina. In: *StatPearls*," *Treasure Island (FL): StatPearls Publishing*, 2023.
- Li W, Li C, Liu L, et al. "Molecular epidemiology of enterovirus from children with herpangina or hand, foot, and mouth disease in Hangzhou, 2016," *Archives of Virology*, vol. 164, no. 10, pp. 2565-2571, 2019.
- Takechi M, Fukushima W, Nakano T, et al. "Nationwide Survey of Pediatric Inpatients With Hand, Foot, and Mouth Disease, Herpangina, and Associated Complications During an Epidemic Period in Japan: Estimated Number of Hospitalized Patients and Factors Associated With Severe Cases," *Journal of Epidemiology*, vol. 29, no.9, pp. 354-362, 2019.
- Ye YZ, Dou YL, Hao JH, et al. "Efficacy and safety of interferon α -2b spray for herpangina in children: A randomized, controlled trial," *International Society for Infectious Diseases*, vol. 107, pp. 62-68, 2021.
- Yu H, Li XW, Liu QB, et al. "Diagnosis and treatment of herpangina: Chinese expert consensus," *World Journal of Pediatrics*, vol. 16, no. 2, pp. 129-134, 2020.
- Lang X, Wang Y, Wang X, et al. "Clinical observation of infantile herpetic angina treated with acupuncture:a randomized controlled trial," *Zhongguo Zhen Jiu*, vol. 37, no. 6, pp. 613-616, 2017.
- Zhang S, Cui Y, Zhou X, et al. "Efficacy of acupuncture on acute pharynx infections: A systematic review and meta-analysis," *Medicine (Baltimore)*, vol. 102, no. 25, pp. e34124, 2023.
- Huang CC, Kotha P, Tu CH, et al. "Acupuncture: A Review of the Safety and Adverse Events and the Strategy of Potential Risk Prevention," *American Journal of Chinese Medicine*. 2024.
- Nicholson JK, Lindon JC, Holmes E. "Metabonomics': understanding the metabolic responses of living systems to pathophysiological stimuli via multivariate statistical analysis of biological NMR

- spectroscopic data,” *Xenobiotica*, vol. 29, no. 11, pp. 1181-1189, 1999.
15. Wang R, Shi L, Liu S, et al. “Mass spectrometry-based urinary metabolomics for the investigation on the mechanism of action of *Eleutherococcus senticosus* (Rupr. & Maxim.) Maxim. leaves against ischemic stroke in rats.” *Journal of Ethnopharmacology*, vol. 241, pp. 1181-118111969, 2019.
 16. Muthubharathi BC, Gowripriya T, Balamurugan K. “Metabolomics: small molecules that matter more,” *Molecular Omics*, vol. 17, no. 2, pp. 210-229, 2021.
 17. Pedley AM, Benkovic SJ. “A New View into the Regulation of Purine Metabolism: The Purinosome,” *Trends in Biochemical Sciences*, vol. 42, no. 2, pp. 141-154, 2017.
 18. Huang S, Liang H, Chen Y, et al. “Hypoxanthine ameliorates diet-induced insulin resistance by improving hepatic lipid metabolism and gluconeogenesis via AMPK/mTOR/PPAR α pathway,” *Life Sciences*, vol. 357, pp. 123096, 2024.
 19. Dang D, Zhang C, Zhang R, et al. “Involvement of inducible nitric oxide synthase and mitochondrial dysfunction in the pathogenesis of enterovirus 71 infection,” *Oncotarget*, vol. 8, pp. 81014–81026, 2017.
 20. Cheng ML, Weng SF, Kuo CH, Ho, et al. “Enterovirus 71 induces mitochondrial reactive oxygen species generation that is required for efficient replication,” *PLoS One*, vol. 9, pp. e113234, 2014.
 21. Ames BN, Cathcart R, Schwiers E, et al. “Uric acid provides antioxidant defense in humans against oxidant - and radical -caused aging and cancer: a hypothesis,” *Proceedings of the National Academy of Sciences of the United States of America*, vol. 78, no. 11, pp. 11, 1981.
 22. Hink HU, Fukai T. “Extracellular superoxide dismutase, uric acid, an atherosclerosis,” *Cold Spring Harbor Symposia on Quantitative Biology*, vol. 67, pp. 483-490, 2002.
 23. Arnold PK, Finley LWS. “Regulation and function of the mammalian tricarboxylic acid cycle.” *Journal of Biological Chemistry*, vol. 299, no. 2, pp. 102838, 2023.
 24. Sánchez-García FJ, Pérez-Hernández CA, Rodríguez-Murillo M, et al. “The Role of Tricarboxylic Acid Cycle Metabolites in Viral Infections,” *Frontiers in Cellular and Infection Microbiology*, vol. 11, pp. 725043, 2021.
 25. Ryan DG, O’Neill LAJ. “Krebs cycle rewired for macrophage and dendritic cell effector functions,” *FEBS Letters*, vol. 591, pp. 2992–3006, 2017.
 26. Noe JT, Mitchell RA. “Tricarboxylic acid cycle metabolites in the control of macrophage activation and effector phenotypes,” *Journal of Leukocyte Biology*, vol. 106, pp. 359–67, 2019.
 27. Ma H, Gao L, Chang R, et al. “Crosstalk between macrophages and immunometabolism and their potential roles in tissue repair and regeneration,” *Heliyon*, vol. 10, no. 18, pp. e38018, 2024.
 28. Yang Y, Cui BB, Li J, et al. “Tricarboxylic acid cycle metabolites: new players in macrophage,” *Inflammation Research*, vol. 73, no. 4, pp. 531-539, 2024.
 29. Wang F, Zhang S, Vuckovic I, et al. “Glycolytic stimulation is not a requirement for M2 macrophage differentiation,” *Cell Metabolism*, vol. 28, no. 463–475, pp. e464, 2018.
 30. Kelly B, O’Neill LA. “Metabolic reprogramming in macrophages and dendritic cells in innate immunity,” *Cell Research*, vol. 25, pp. 771–84, 2015.
 31. Proffitt C, Bidkhorji G, Lee S, et al. “Genome-scale metabolic modelling of the human gut microbiome reveals changes in the glyoxylate and dicarboxylate metabolism in metabolic disorders,” *iScience*, vol. 25, no. 7, pp. 104513, 2022.
 32. Viola A, Munari F, Sánchez-Rodríguez R, et al. “The Metabolic Signature of Macrophage Responses.” *Frontiers in Immunology*, vol. 10, pp. 1462, 2019.
 33. Yang L, Chu Z, Liu M, et al. “Amino acid metabolism in immune cells: essential regulators of the effector functions, and promising opportunities to enhance cancer immunotherapy,” *Journal of Hematology & Oncology*, vol. 16, no. 1, pp. 59, 2023.
 34. Wu G. “Amino acids: metabolism, functions, and nutrition,” *Amino Acids*, vol. 37, no. 1, pp. 1-17, 2009.
 35. Brosnan ME, Brosnan JT. “Histidine Metabolism and Function,” *Journal of*

- Nutrition*, vol. 150, no. Suppl 1, pp. 2570S-2575S, 2020.
36. Wang SM, Lei HY, Liu CC. "Cytokine immunopathogenesis of enterovirus 71 brain stem encephalitis," *Clinical and Vaccine Immunology*, vol. 2012, pp. 876241, 2012.
37. Sender R, Fuchs S, Milo R. "Are We Really Vastly Outnumbered? Revisiting the Ratio of Bacterial to Host Cells in Humans," *Cell*, vol. 164, no. 3, pp. 337-340, 2016.
38. Kayama H, Okumura R, Takeda K. "Interaction Between the Microbiota, Epithelia, and Immune Cells in the Intestine," *Annual Review of Immunology*, vol. 38, no. 23-48, pp. 337-340, 2020.
39. Fritz JH. "Arginine cools the inflamed gut," *Infection and Immunity*, vol. 81, no. 10, pp. 3500-3502, 2013.
40. Nüse B, Holland T, Rauh M, et al. "L-arginine metabolism as pivotal interface of mutual host-microbe interactions in the gut," *Gut Microbes*, vol. 15, no. 1, pp. 2222961, 2023.
41. Moriguchi T, Takai J. "Histamine and histidine decarboxylase: Immunomodulatory functions and regulatory mechanisms," *Genes to Cells*, vol. 25, no. 7, pp. 443-449, 2020.
42. Walter M, Kottke T, Stark H. "The histamine H₄ receptor: targeting inflammatory disorders," *European Journal of Pharmacology*, vol. 668, no. 1-2, pp. 1-5, 2011.
43. Yamayoshi S, Yamashita Y, Li J, et al. "Scavenger receptor B2 is a cellular receptor for enterovirus 71," *Nature Medicine*, vol. 15, no. 7, pp. 798-801, 2009.
44. Zhou D, Zhao Y, Kotecha A, et al. "Unexpected mode of engagement between enterovirus 71 and its receptor SCARB2," *Nature Microbiology*, vol. 4, no. 3, pp. 414-419, 2019.
45. Huang YL, Lin TM, Wang SY, et al. "The role of conserved arginine and proline residues in enterovirus VP1 protein," *Journal of Microbiology Immunology and Infection*, vol. 55, no. 4, pp. 590-597, 2022.